Studies of the Inter-ELM Pedestal Instabilities Modulated by Bursts on DIII-D

A. Diallo[1], J. Dominski[1], K. Barada[2], F. Laggner[1], M. Knolker[1], G.J. Kramer[1], T.L. Rhodes[2], L. Zeng[2], and G. McKee[3]

[1] *Princeton Plasma Physics Laboratory, P.O. 451, Princeton, NJ, USA*

[2] *Physics Department, University of California Los Angeles, Los Angeles, CA, USA*

[3] *University of Wisconsin-Madison, 1500 Engineering Dr., Madison, WI, USA*

Understanding the physics leading to the onset of edge-localized-modes (ELM) is an active and critical area of edge physics research for ITER projections. The leading model explaining the onset of type I ELM[1;2] is centered around the peeling ballooning (PB) magnetohydrodynamic (MHD) instability[3]. In this theory the edge pressure gradient and edge current density grow in the inter-ELM period until the PB stability boundary is crossed at which point the ELM is triggered. While ultimately it might be that the PB mode leads to the type I ELM onset, the edge parameters can exist near this unstable region for a substantial part of the inter-ELM period. During such inter-ELM period, there is growing experimental evidence[4;5;6;7] showing pedestal instability activities correlated with the pedestal parameters dynamics, in which the pedestal gradients appear to be pinned to the linear marginally stable ballooning profiles or microtearing modes prior to ELM onset. To improve our understanding of the ELM onset, we focus on the inter-ELM phase leading up to the ELM onset.

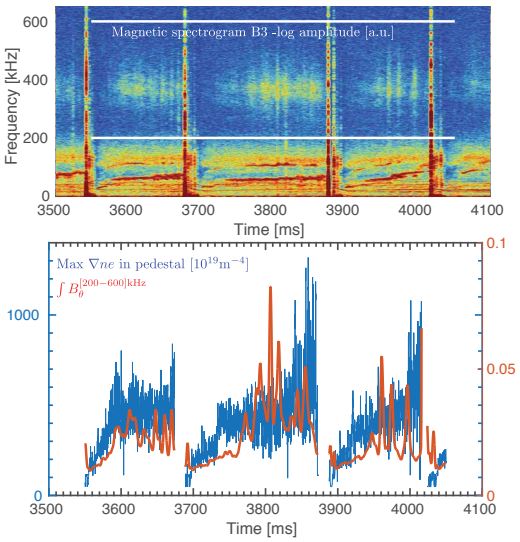

Figure 1: Top panel: Magnetic spectrogram shows the intermittent bursts (#170869). Bottom panel: Time history of the density gradient evolution and integrated spectral power of the magnetic fluctuations.

We report on analysis of type I ELMy discharge (170869) in DIII-D (LSN, q_{95} varying from 3.4 to 5) during the inter-ELM phase where intermittent bursting activities of a high frequency pedestal modes have been observed. Specifically, we characterize the bursts, and analyze their effects on pedestal transport. We show a preliminary nonlinear analysis to develop an understanding of the trigger of these bursts.

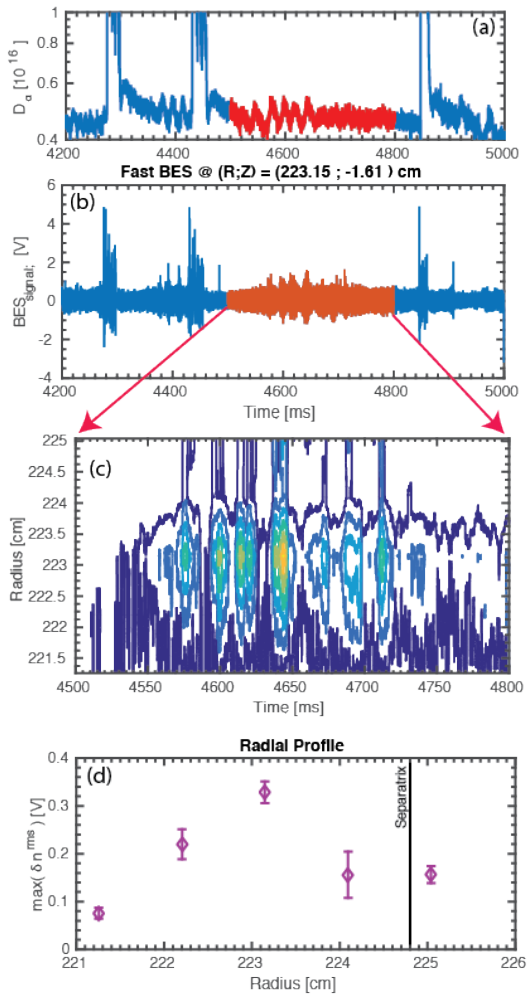

Figure 2: Localization of the bursts using BES analysis. (a) Time history of D_α trace with the bursts. (c) Fast BES signal with bursts. (c) RMS amplitude of BES bursts at various radii. (d) Radial profile of a burst, measured with density fluctuations from BES.

Fig. 1 displays in the top panel the magnetic spectrogram showing the high frequency mode ($\sim$ 390kHz) being modulated in bursts during the inter-ELM phase. In the bottom panel of Fig. 1, we show the comparison between the mode amplitude dynamics (averaged between 200 - 600 kHz) and the density gradient evolution, suggesting a density gradient driven mode (not shown here). It is this underlying mode that is modulated by the bursts. Note that these bursting activities (bursts are the vertical spikes in the top panel of Fig 1 between ELMs) are remarkably similar to observations on the JET ILW inter-ELM magnetic activities (see Fig. 15 of Ref.[8]). Similarly, strong intermittent density fluctuation bursts are observed between the ELMs on AUG[9]. We also show below that these bursts are similar to the bursting modes observed in the BES signal of enhanced H-mode pedestal with lithium injection in DIII-D[10].

Fig. 2(a) displays the effects of the bursts on D_α trace (these bursts are the same as those in Fig 1). We utilize the BES diagnostic (see Fig. 2(b) for an example time trace) to localize the bursts to the pedestal. Fig. 2(c) displays the contour plot of the rms density fluctuations due to these bursts for various BES radii. The radial profile of the max rms is shown in Fig. 2(d), clearly indicating that these bursts are localized in the pedestal. The bursts are also localized below the midplane (not shown here) in the poloidal direction.

This radial localization is confirmed using the Doppler back scattering (DBS) system. Figs. 3(a) and (b) show the signatures of the bursts on the D_α trace and on the magnetic probes, respectively. Fig. 3(c) represents the frequency cutoffs, along with Fig. 3(d) and (e) that display the DBS quadrature spectrograms for two radial locations sampling the bottom and middle of the pedestal. It is clearly observed from the top spectrogram (Fig. 3(d)) that the bursts are localized in the middle of the pedestal. These DBS measurements extend the BES analysis results to higher wavenumber.

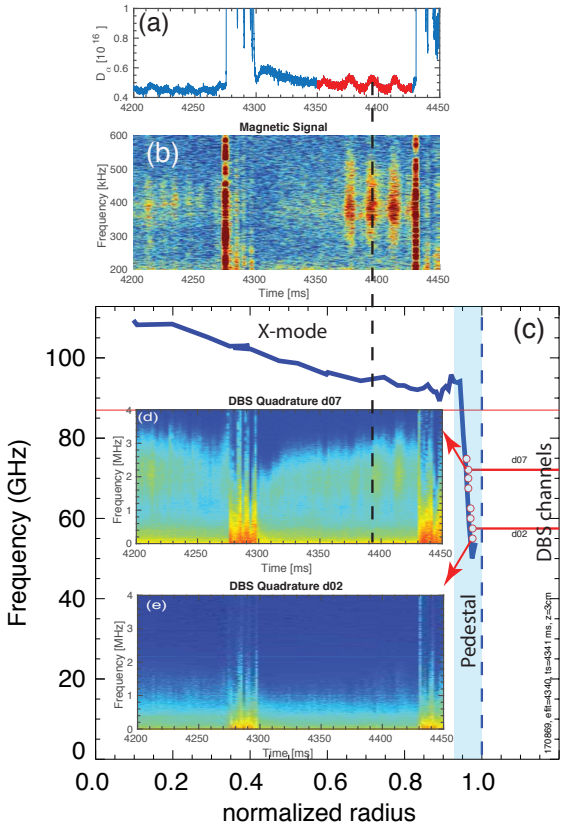

Figure 3: (a) Time history of D_α with the region of interest highlighted in red. (b) Magnetic spectrogram indicating the high frequency modulated by the bursts. (c) Frequency cutoff of the X-mode DBS system showing the localization (the open circles) of the measurements in the pedestal. (d) DBS Quadrature spectrogram showing the bursts aligned with the magnetic signal burst located at mid-pedestal. (e) DBS Quadrature spectrogram showing the foot of the pedestal.

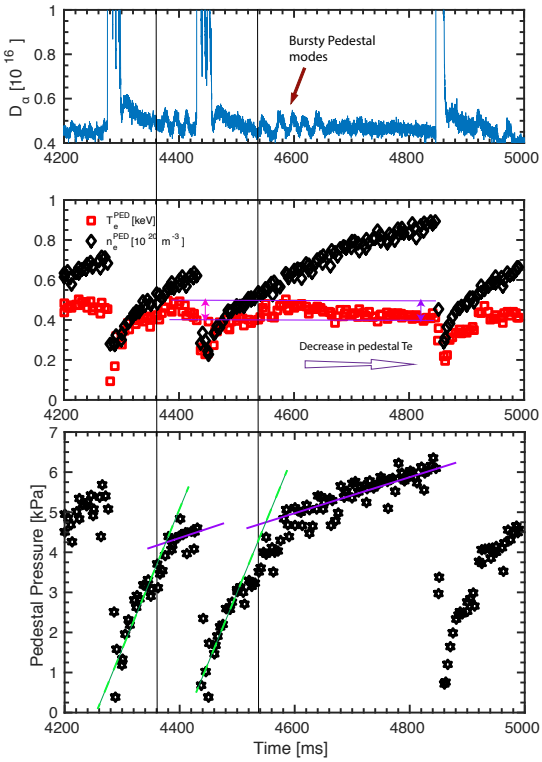

Figure 4: Burst and electron pedestal parameters. Top panel: Time history of the D_α with bursts signatures. Middle panel: The pedestal density and temperature evolution between ELMs. The temperature pedestal evolution altered when the bursts kick in, while the density pedestal evolution continues to evolve until the next ELM. Bottom panel: the pressure pedestal evolution.

We now investigate the transport effects due to these bursts. The top panel of Fig. 4 indicates the burst of D_α with the vertical lines representing onsets of the bursts. In the middle panel of Fig. 4, we show the time evolution of the electron density and temperature pedestals. In this panel, we indicated the vertical lines where the bursts become noticeable on the D_α trace, shortly after which the pedestal temperature starts to droop as one approaches the end of the ELM cycle (see lines indicating the droop in Fig. 4). However, the bursts have no effects on the inter-ELM evolution of the pedestal density. The bottom panel of Fig. 4 displays the electron pedestal pressure with a change in the evolution of the trajectory when the bursts are triggered. Overall, Fig. 4 is consistent with bursts causing electron heat transport in the pedestal.

Above, we have shown that the bursts are intermittent and appear to only be modulating the high frequency mode (200 - 600 kHz as bracketed by the horizontal lines in the top panel of Fig 1) similar to observations on other devices. This mode's onset appears to be correlated with the pedestal density gradient evolution. The bursts were shown to be localized in the pedestal using BES and DBS systems, consistent with AUG observa-

tions[9] and burst activities in Ref.[10]. Finally, it is clear from time history of the pedestal temperature, density and pressure, that the bursts have strong effects on the temperature pedestal evolution between ELMs. Thus, the electron heat channel is predominantly affected by these bursts.

Given the characterization of the bursts above and the intermittent nature, we investigate possible nonlinear interactions of pedestal modes leading to the bursts. Fig. 5(a) displays a zoomed in version of the magnetic spectrogram where the bursts are observed. We confirmed that these bursts are not correlated with the neutral beam modulations. Fig. 5(b) represents the power spectra of the magnetic signal for two selected times with and without the bursts. One useful tool, enabling analyses of the nonlinear coupling between modes and the energy transfer, is the bicoherence b^2 applied to the magnetic signal (referred to as S). The bicoherence b^2 is defined by equation (see Ref.[11]): $b^2 = \frac{|\langle S_{f_1} S_{f_2} S^*_{f_1+f_2}\rangle|^2}{\langle |S_{f_1} S_{f_2}|^2\rangle \langle |S_{f_1+f_2}|^2\rangle}$, where S_f is the signal evaluated at frequency f and S^*_f its complex conjugate. Fig. 5(c) and (d) display the bicoherence with and without the bursts. The bursts near 350 kHz appear to result from nonlinear interactions between low frequency ubiquitous quasi-coherent modes during the inter-ELM phase (as reported in AUG[6], DIII-D[7], JET[4]). Future work will identify the possible triads systematically leading to the bursts as well as their combined effects on transport.

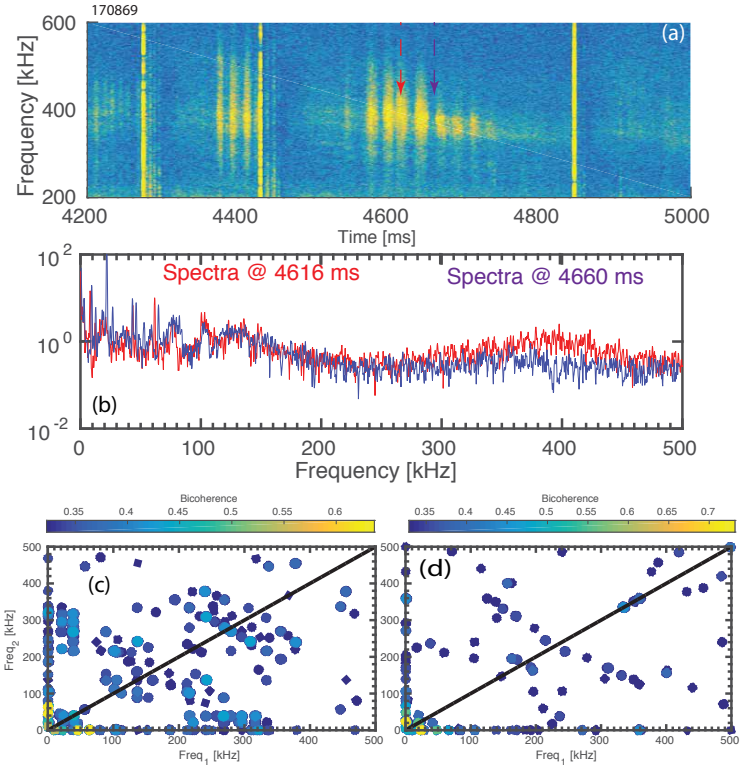

Figure 5: Nonlinear analysis.(a) Magnetic spectrogram show the high frequency mode modulated by the bursts. The two arrows indicate region with and without the bursts. (b) Power spectra with and without the bursts. (c) Bicoherence when the bursts are ON. (d) Bicoherence when the bursts are OFF.

This work has been supported by the U.S. DOE under the Contracts No.DE-FC02-04ER54698, DE-AC02-09CH11466, DE-FG02-08ER54999, and DE-FG02-08ER54984. **Disclaimer**: This report was prepared as an account of work sponsored by an agency of the United States Government. Neither the United States Government nor any agency thereof, nor any of their employees, makes any warranty, express or implied, or assumes any legal liability or responsibility for the accuracy, completeness, or usefulness of any information, apparatus, product, or process disclosed, or represents that its use would not infringe privately owned rights. Reference herein to any specific commercial product, process, or service by trade name, trademark, manufacturer, or otherwise does not necessarily constitute or imply its endorsement, recommendation, or favoring by the United States Government or any agency thereof. The views and opinions of authors expressed herein do not necessarily state or reflect those of the United States Government or any agency thereof.

[1] H Zohm *Plasma Phys. Control. Fusion*, 38:105, 1996.
[2] A. W. Leonard *Physics of Plasmas (1994-present)*, 21(9):–, 2014.
[3] J W Connor *Plasma Physics and Controlled Fusion*, 40(5):531, 1998.
[4] C P Perez *et al.*, *Plasma Physics and Controlled Fusion*, 46(1):61, 2004.
[5] A. Diallo *et al.*, *Phys. Rev. Lett.*, 112:115001, Mar 2014.
[6] F M Laggner *et al. Plasma Physics and Controlled Fusion*, 58(6):065005, 2016.
[7] A. Diallo *et al.*, *Physics of Plasmas (1994-present)*, 22(5):–, 2015.
[8] C. Bowman *et al.*, *Nuclear Fusion*, 58(1):016021, 2018.
[9] P. Hennequin *et al.*, In *44th EPS Conf. on Plasma Physics*, number PI.167, 2017.
[10] T.H. Osborne *et al.*, *Nuclear Fusion*, 55(6):063018, 2015.
[11] Ch. P. Ritz *et al.*, *Physics of Fluids B: Plasma Physics*, 1(1):153–163, 1989.